CHAPTER V

IDENTIFICATION OF CONTROL LAWS IN HUMAN STANDING BALANCE

Conference Abstract:

1. STANDING BALANCE CONTROL PARAMETER IDENTIFICATION WITH DIRECT COLLOCATION. Dynamic Walking 2016.
2. CONTROLLER IDENTIFICATION IN HUMAN STANDING BALANCE. Dynamic Walking 2018.

ABSTRACT

Controller identification of standing balance is a well known research question. However, engineering applicable parametric controllers haven't been identified. In this paper, we identified stable standing balance controller from long period experiment data under random perturbations. Five controller types, from simple to complex, were identified in this paper. Eigenvalues were calculated of the identified controllers. Results shows that five out off six participants have similar eigenvalues, which means similar system reactions.

5.1 Introduction

Feedback control, instead of preprogramed posture strategies, has been accepted to control posture in human standing balance task [1]. Although studies have been conducted trying to understand the feedback control system, controllers have not been got directly from human standing balance experiment data that could be applied on engineering devices, for instance, humanoid robots and P/O devices.

In optimal control aspect, studies have tried to design optimal controllers in the frame work of balance strategies in how human keep balance [1–3]. For example, in the framework of ankle & Hip strategies, optimal feedback controllers were designed using linear quadratic regulator (LQR) [4]. In simulation, these designed optimal controllers can keep human model (two-link pendulum) balance under external perturbations. However, their performances is different from how human reacts to perturbation.

CoM and Cop are the two important information when studies trying to explain the criteria that how human stay standing balance. It has been accepted that in order to keep standing balance, in general, CoP is suggested to stay inside the support area (area defined by the out curves of two feet) [5, 6]. However, how human keep Cop inside the support area is

still unclear with this research direction.

To understand how human use feedback control to keep standing balance, studies have been done to identify controllers from human standing balance experimental data [7–11]. In experiments, subjects were either perturbed with extra force, or the standing platform has a unexpected motion. The indirect identification approach is mostly used in these identification studies , since the open-loop identification will introduce bias [12].For instance, Park et al. identified stable full states PD controller parameters in different amplitudes of perturbations. It is concluded that the controller gains are changing along with the ramp perturbation amplitudes [7]. Welch et al. used ramp perturbation also to identify muscle activation [8, 13]. Kiemel et al. identified the non-parametric neural feedback of the standing balance under mechanical perturbation. The identified results suggested that human tends to keep stability rather than minimize sway [9]. Perterka and van der Kooji identified non-parametric motor-sensor control information from experiment data in frequency domain. They used continually perturbation and linear controller structures [10, 14, 15]. Goodworth et al. tested the identification method on simulation data in frequency domain, but have not reported results on human experiment data [11]. Although all these studies has been done, there is no engineering applicable controllers that has been extracted.

In this study, we proposed that there exists common general feedback controllers among healthy human to keep standing balance. Here, general means controller parameters do not change according to perturbation characters. In the chapter, We will identify the common control laws of healthy human standing balance. The identification will be done in time domain, which can be directly applied to engineering use. In order to identify this general controller, we applied long period continuous perturbation in experiment to collect how healthy human response to it. Linear and nonlinear control laws were identified in the chapter. Section 2 will describe the method used for identification. Experiment process

and data which used for identification were described in Chapter II. Section 3 shows identified results. Section 4 discusses the identified results. Conclusion and future work are mentioned in section 5.

5.2 Methods

In this section, identification approach, human body dynamics, controller types are described.

5.2.1 Indirect Approach

An indirect identification approach was used in this study to avoid the bias of direct identification [12]. In the indirect approach, a closed-loop system including human body dynamics, feedback controller were built to represent the human standing balance system. Since ankle and hip strategies are mainly used in keeping standing balance, human body dynamics was simplified to a double inverted pendulum model. Feedback controllers were used to control the motions of ankle and hip joint. Control parameters in the feedback controller were the targets of the identification. The indirect identification approach can be treated as an optimization problem, in which control parameters are optimized by minimizing the difference between the model output and the experiment data. The best control parameters are those who can make the close-loop model generate the same motion with experiment data under the same perturbation. The diagram of the indirect identification approach is shown in Figure 20.

More specifically, the optimization problem mentioned above is a trajectory optimization problem. To make it efficient, direct collocation method, other than shooting method, is used in this work. It has been shown that that direct collocation method is more efficient in trajectory optimization [16]. Here, direct collocation is used with 50 collocation nodes per second. Ipopt solver is used to solve optimization problems.

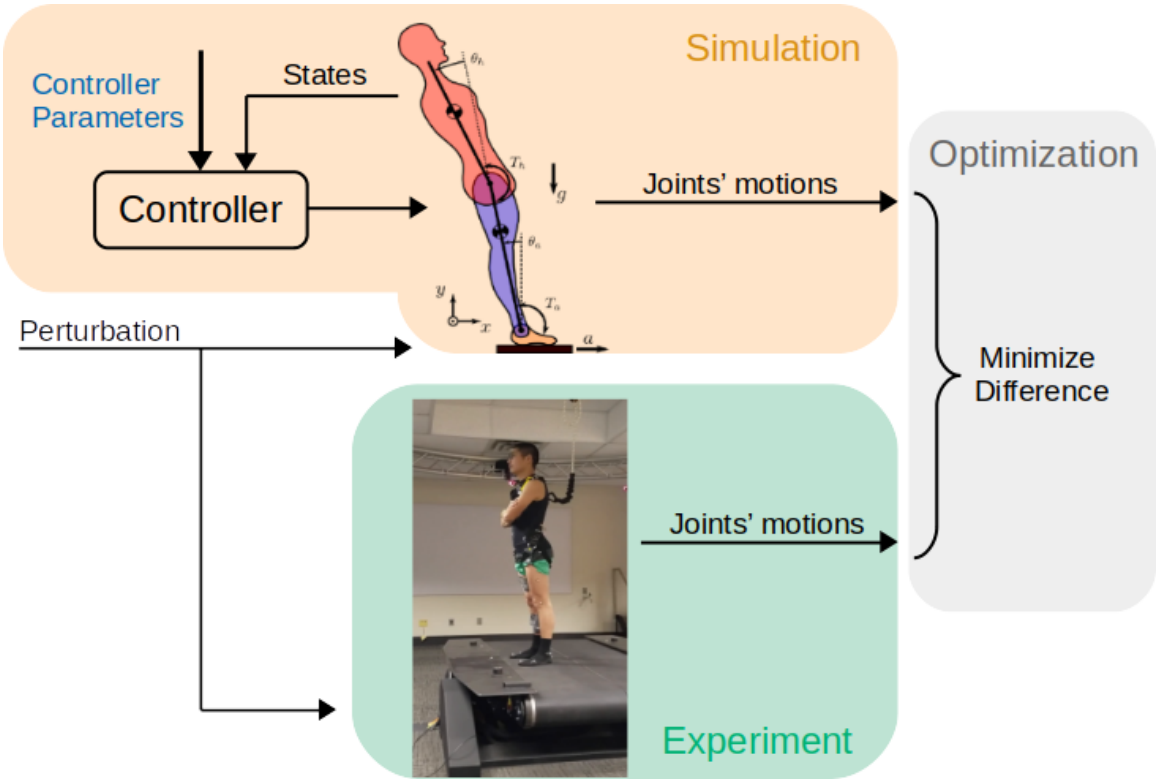

Figure 20: Structure of indirect identification approach in standing balance task. Identification can be treated as an optimization problem, in which control parameters are optimized by minimizing the difference between the model output and the experiment data

5.2.2 Human Body Dynamics

In the experiment, feet of participants were always rigidly attached with the ground. Therefore, human body dynamics is simplified to a double-link pendulum with foot combined with standing plate. The double-link pendulum is also a two dimensional model, since perturbation was only applied on sagittal plane. The segments lengths, mass, inertia were calculated based on participants' height and weight using the anthropometry table in Winter's book[17]. Dynamic equations of the double-link pendulum were generated using *Python Sympy* package[18].

5.2.3 Controller Structures

Five types of feedback controllers were used in this paper to identify control parameters on the experiment data mentioned in Chapter II. Two of them are linear: proportional-derivative (PD) controller and full-states proportional-derivative (FPD) controller. The other three are nonlinear: linear states combination with time delay (LSCTD) controller, neural network (NN) controller, and neural network with time delay (NNTD) controller. The formulas of these five controllers are shown below.

PD controller:

$$\begin{bmatrix} T_a(t) \\ T_h(t) \end{bmatrix} = \begin{bmatrix} K_{p_a} & 0 & K_{d_a} & 0 \\ 0 & K_{p_h} & 0 & K_{d_h} \end{bmatrix} \begin{bmatrix} \theta_a(t) - \theta_a^{ref} \\ \theta_h(t) - \theta_h^{ref} \\ \dot{\theta}_a(t) \\ \dot{\theta}_h(t) \end{bmatrix} \tag{5.1}$$

FPD controller:

$$\begin{bmatrix} T_a(t) \\ T_h(t) \end{bmatrix} = \begin{bmatrix} K_{p_{aa}} & K_{p_{ah}} & K_{d_{aa}} & K_{d_{ah}} \\ K_{p_{ha}} & K_{p_{hh}} & K_{d_{ha}} & K_{d_{hh}} \end{bmatrix} \begin{bmatrix} \theta_a(t) - \theta_a^{ref} \\ \theta_h(t) - \theta_h^{ref} \\ \dot{\theta}_a(t) \\ \dot{\theta}_h(t) \end{bmatrix} \tag{5.2}$$

LSCTD Controller:

$$\begin{bmatrix} T_a(t) \\ T_h(t) \end{bmatrix} = \sum_{m=0}^{D} \left(\begin{bmatrix} K_{p_{aa}}^m & K_{p_{ah}}^m & K_{d_{aa}}^m & K_{d_{ah}}^m \\ K_{p_{ha}}^m & K_{p_{hh}}^m & K_{d_{ha}}^m & K_{d_{hh}}^m \end{bmatrix} \begin{bmatrix} \theta_a(t - m * \delta t) - \theta_a^{ref} \\ \theta_h(t - m * \delta t) - \theta_h^{ref} \\ \dot{\theta}_a(t - m * \delta t) \\ \dot{\theta}_h(t - m * \delta t) \end{bmatrix} \right) \tag{5.3}$$

where $T_a(t)$ is ankle joint torque at time point t and $T_h(t)$ is hip joint torque at time point t; $\theta_a(t)$ and $\theta_h(t)$ are ankle and hip joint angles at time point t; $\dot{\theta}_a(t)$ and $\dot{\theta}_h(t)$ are ankle and hip joint angular velocities at time point t; $\theta_a(t-m*\delta t)$ and $\theta_h(t-m*\delta t)$ are ankle and hip joint angles at m^{th} point prior to the current time point t; $\dot{\theta}_a(t - m * \delta t)$ and $\dot{\theta}_h(t - m * \delta t)$ are ankle and hip joints angular velocities at m^{th} point prior to the current time point t; K_p and K_d are proportional and derivative gains of feedback controllers multiplied with the state at time point t. K_p^m and K_d^m are proportional and derivative gains of feedback controllers multiplied with the state at m^{th} point prior to the current time point t.

NN Controller:

NN controller was defined as standard neural network with one hidden layer and four hidden nodes. It is nonlinear controller, since its activation function is a nonlinear function. The inputs of the NN controller are four states and outputs are two torques. Besides, one constant node (unit input) was added at both input and hidden layer. The activation function used in NN controller is smoothed leaky-ReLU function. The reason of smooth is to make

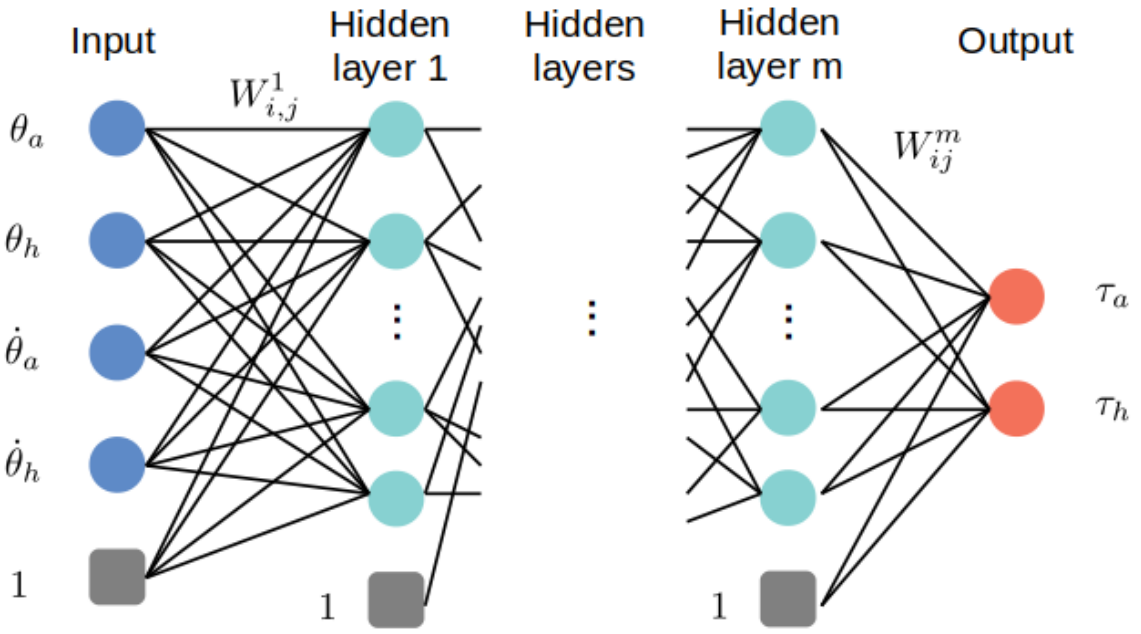

Figure 21: Structure of general neutral network as controller. Control parameters are the weights between layers.

it differentiable at all points. The general structure of neural network is shown in Figure 21. The smoothed activation function is:

$$f(x) = x + 0.7(\frac{x - \sqrt{x^2 + 0.0001}}{2}) \tag{5.4}$$

NNTD Controller:

NNTD controller used the same neural networking settings but with one hidden layer and eight hidden nodes. The difference is that the inputs of the NN controller are four current states and prior states (delay inputs). Outputs of NNTD controller are two torques.

The total number of optimizing parameters in PD, FPD, LSCTD, NN, and NNTD controllers are 6, 10, 34, 30, and 154, respectively.

5.2.4 Avoid Unstable Controllers

In chapter III, stochastic optimization was introduced to avoid identifying unstable controllers. In this identification work, we applied the stochastic optimization on PD and FPD controller identifications. Since complex controller types (with large control parameters) need more episodes in stochastic optimization. The computing power needed for LSCTD, NN, and NNTD are very high. Therefore, stochastic optimization was not applied on these three nonlinear controller types. Even though the identified controllers of these three controller types may not be stable, the fit between simulation model and experiment data can still reveal the ability of different controller types in explaining the human standing balance experiment data.

5.2.5 Summary of the Identification

Five controller structures were identified on six participants mentioned in Chapter II from participant 3 to participant 8. There are two perturbation trials of each participant. Here, we name the identification of one controller type on one perturbation data trial as one identification problem. In total, there are 60 (five controller types and twelve perturbation trials) identification problems in this standing balance controller identification task. In each identification problem of the first four controller types, ten optimizations were done with random initial guesses to avoid local optimum. For NNTD controller type, only one optimization was done for each identification problem, since it takes a long time to solve the optimization. Best identified controller was chosen has the best fit with experiment data inside ten optimizations.

5.3 Results

Coefficient of determination (R^2) of the best identified controllers in 60 identification problems are shown in Figure 22. For NNTD controller type, only several identification problems were succeed due to the difficulty of solving trajectory optimizations with such a

complex controller type. For other controller types, at least one optimization were successful in each identification problem.

One example of the fit between identified trajectories and experiment data (experiment trial 3 of participant 8) is shown in Figure 23 and 24. From simple to complex controller type, fit between simulation model and experiment data is getting better and better.

Since stochastic optimization help identified stable SPD and FPD controllers. The gains of identified controller and their eigenvalues can be studied to understand how healthy subjects control their standing balance under perturbation. Figure 25 and Figure 26 shows parameters and eigenvalues of identified PD controllers. Figure 27 and Figure 28 shows parameters and eigenvalues of identified FPD controllers. Gains in these figures are normalized by participants' body mass.

Gains of identified PD controllers have similar pattern among all participants except participant 7. Proportional gains are larger than derivative gains. Ankle proportional gains are larger than hip proportional gains. Reference angles of identified PD controllers are small, which agree with our expectation. However, the eigenvalues of them have a large variations. Eigenvalues of participant 4 and 7 are totally different from other participants. The rest four participants are not very close neither.

Gains of identified FPD controllers also have similar pattern among all participants except participant 7. The eigenvalues of them have a relative small variation than identified PD controllers. Five participants have close eigenvalues except participant 7.

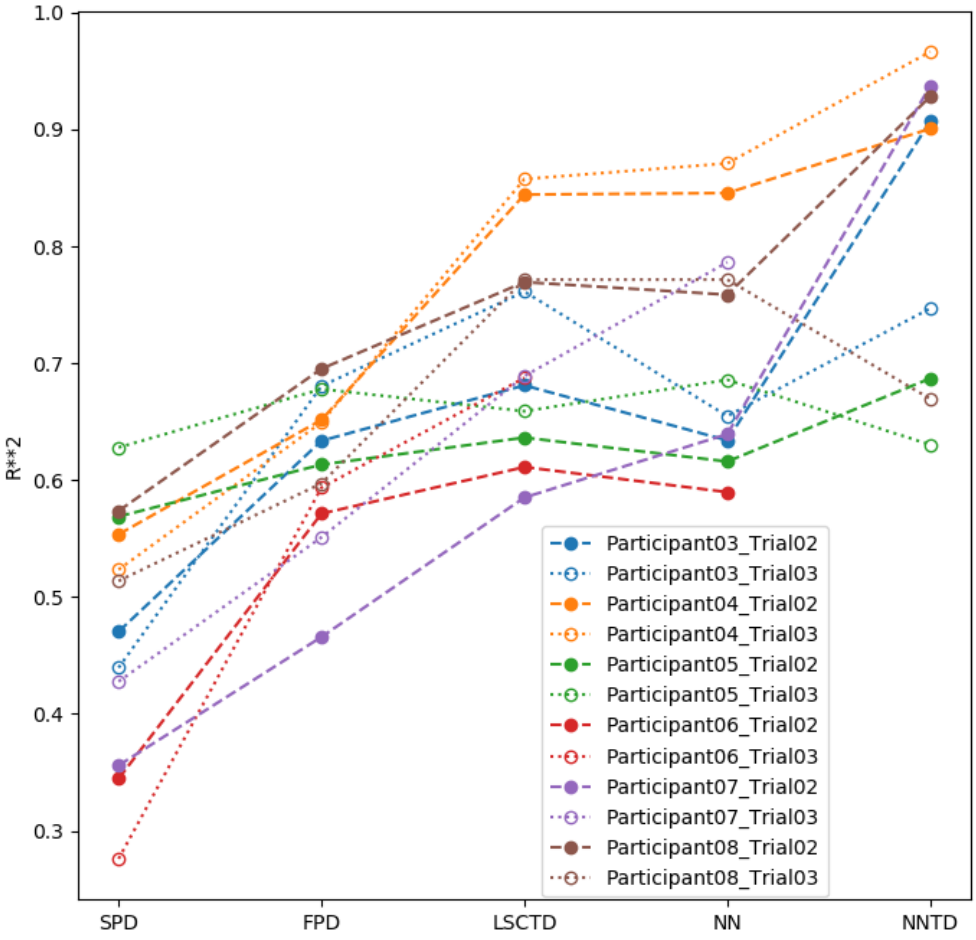

Figure 22: R^2 between the best identified trajectories and experiment data. A higher value means a better fit.

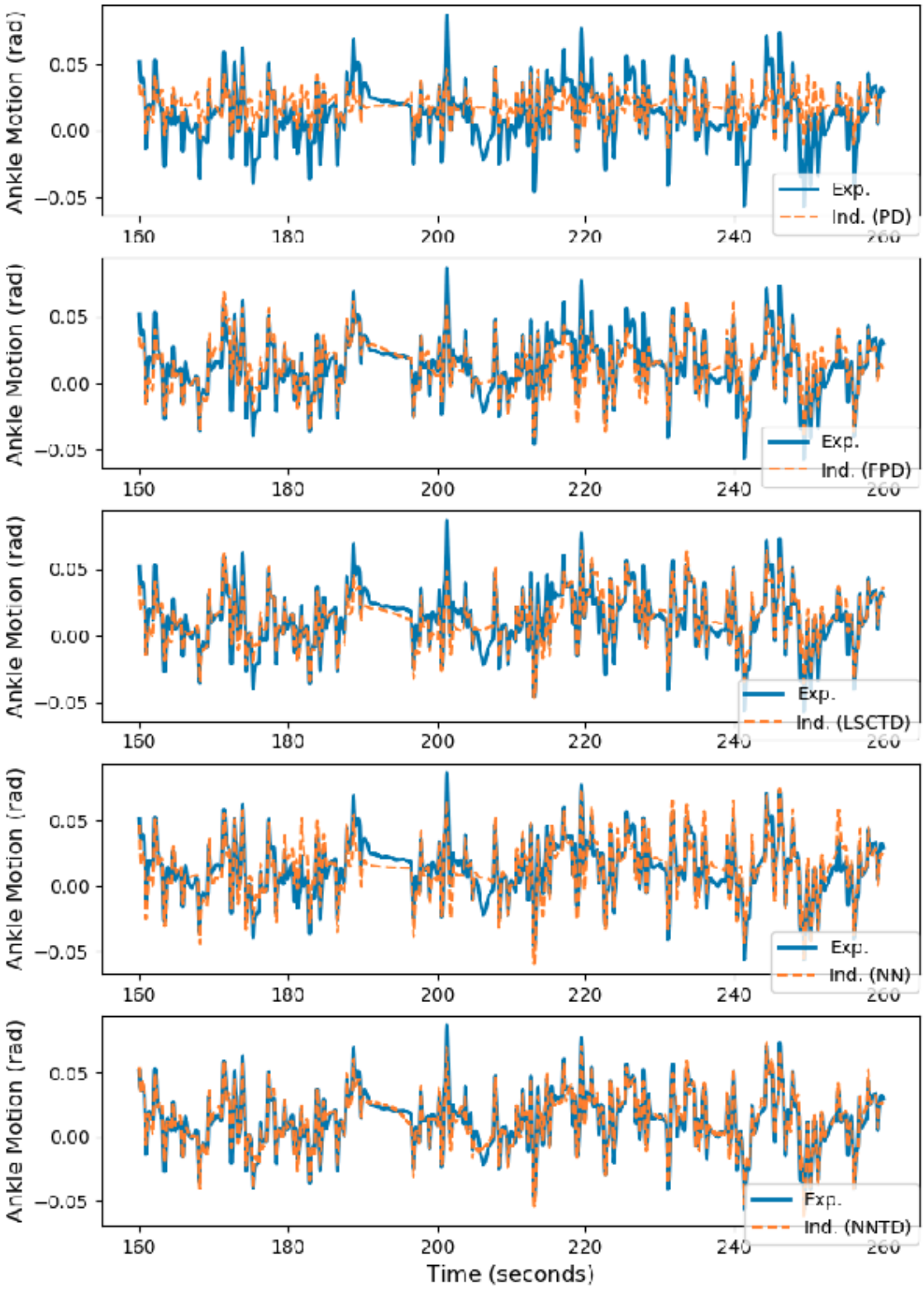

Figure 23: Ankle motion fit of participant 8 and trial 2. Fits get better with more complex controller types

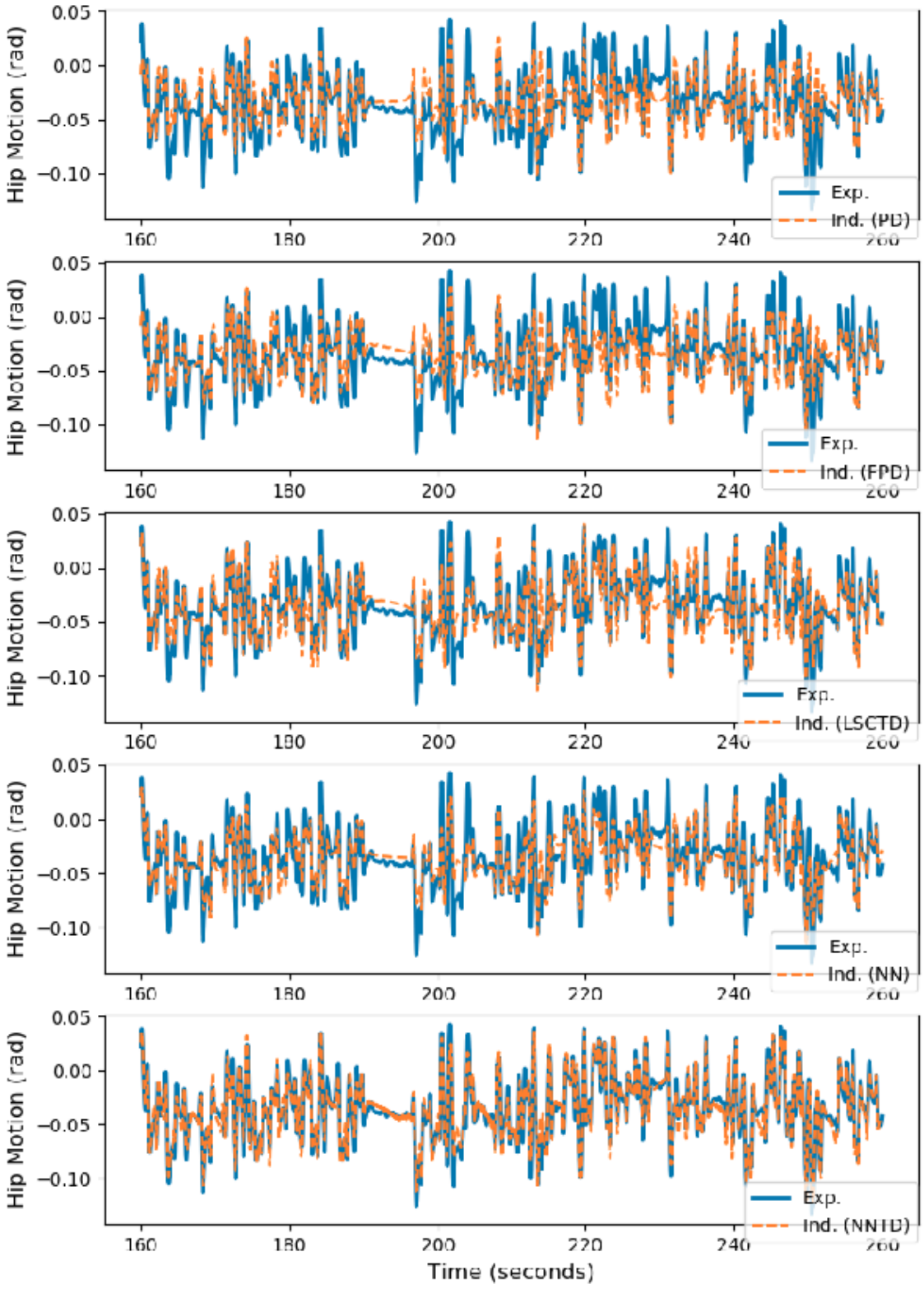

Figure 24: Hip motion fit of participant 8 and trial 2. Fits get better with more complex controller types

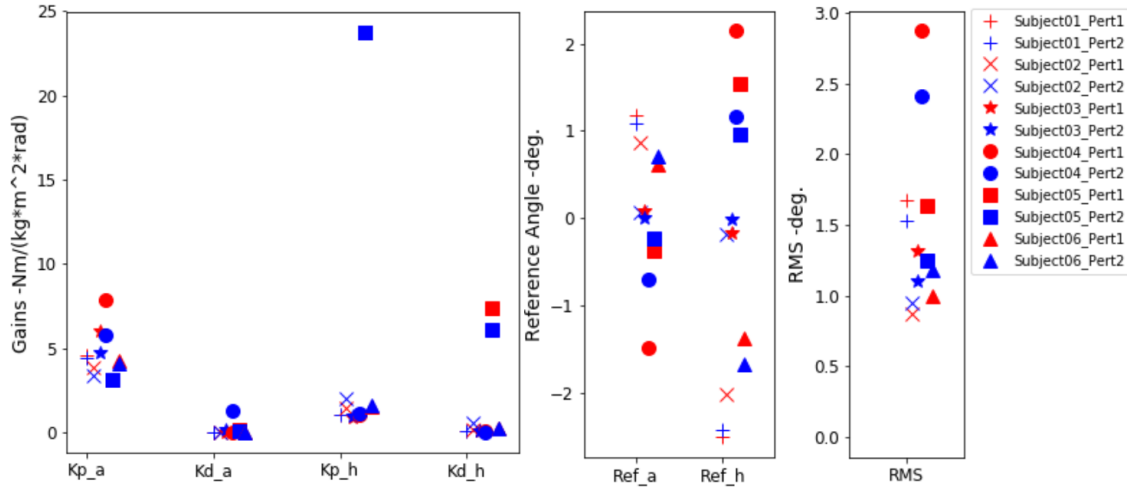

Figure 25: Gains of identified PD controllers of six participants. Five participants have similar gains except participant five.

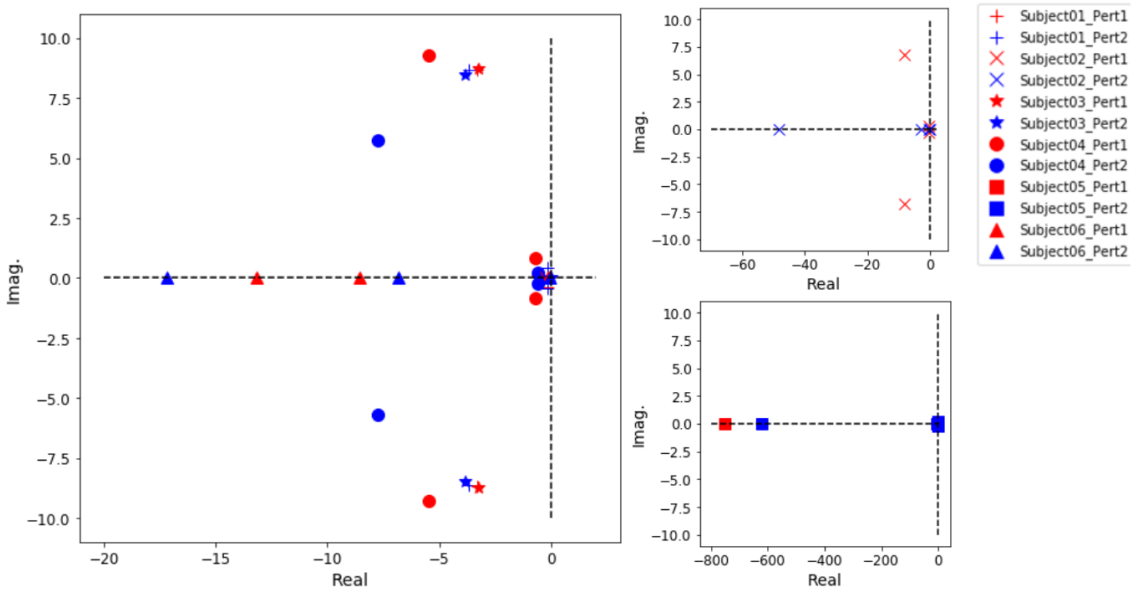

Figure 26: Eigenvalues of identified PD controllers of six participants. They have a large variations.

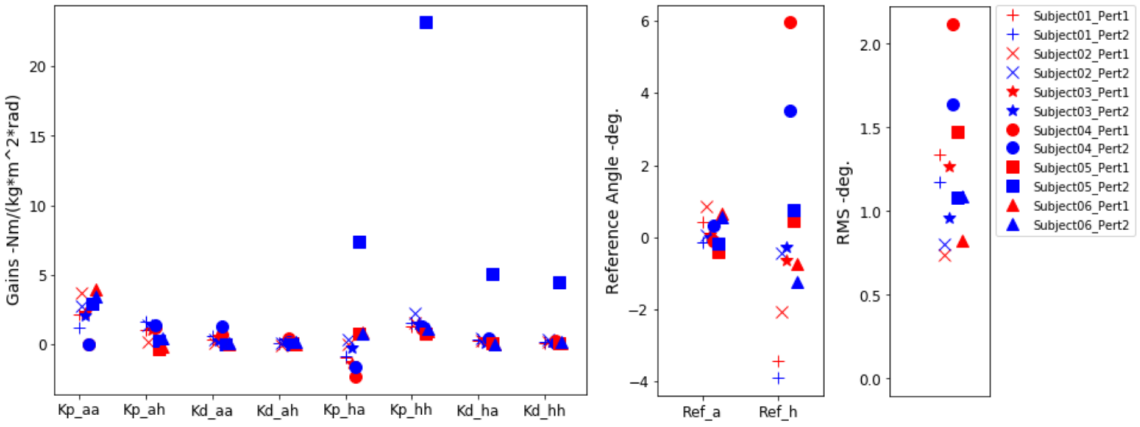

Figure 27: Gains of identified FPD controllers of six participants. Five participants have similar gains except participant five.

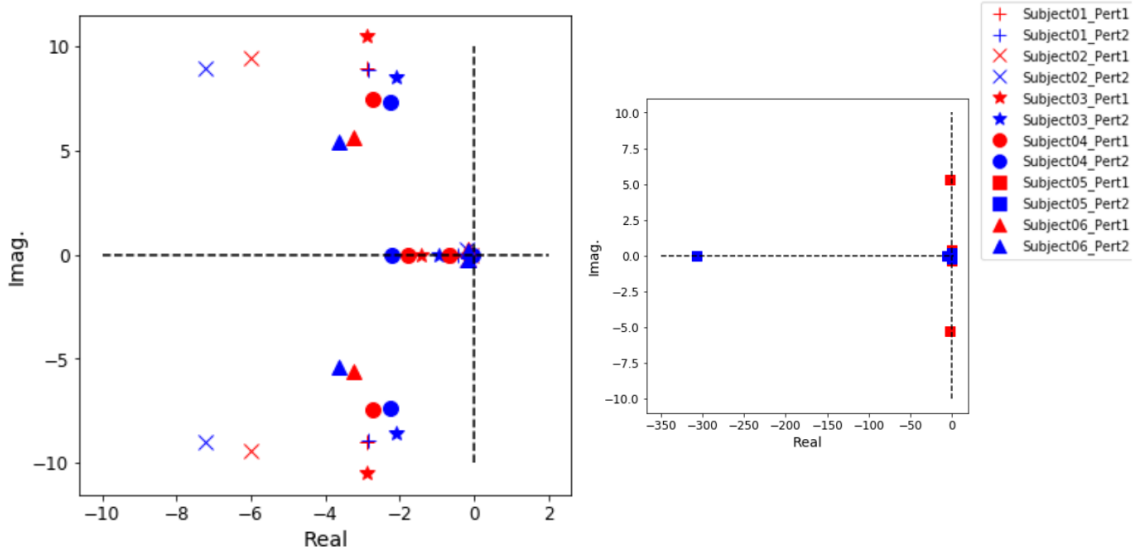

Figure 28: Eigenvalues of identified FPD controllers of six participants. They are closer to each other than identified PD controllers.

5.4 Discussion

The results suggested that a generalized time-invariant feedback controller can explain as long as 100 seconds experiment data under random square wave perturbation. In addition, more complex controller type results a higher fit between identified trajectories and experiment data in general. This is reasonable, since complex controller type has more control parameters which is more powerful in explaining the experiment data.

The mean R^2 of FPD controller type of all identification problems is around 0.6. This is much lower than the R^2 in Park's identification paper [7], in which short ramp perturbation was used. They identified FPD controller on 3 seconds experiment data. This suggested that FPD controller type is not complex enough to generalization and explain long duration balance data.

Identified PD controllers have similar control parameters. Proportional gains are larger than derivative gains, which is reasonable for PD controllers used in position control. Proportional gains of ankle are larger than hip, which means the ankle joint is stiffer than hip in standing balance. This results can be explained by the large torques at ankle joint and small motions during standing balance task. However, identified PD controllers have relatively large difference of system eigenvalues among participants.

Identified FPD controllers have similar control parameters. Proportional gains are larger than derivative gains, which is reasonable for PD controllers used in position control. Proportional gains of ankle are larger than hip, which means the ankle joint is stiffer than hip in standing balance. This results can be explained by the large torques at ankle joint and small motions during standing balance task. Self-state feedback gains are larger than cross-state feedback gains. This means that self-states information are usually used to keep standing balance under perturbation. Identified FPD controllers also have relatively small difference

of system eigenvalues among participants.

5.5 Conclusion

In this chapters, we identified five types of controllers from 100 seconds period standing balance experiment data. Stable controllers were able to identified for two linear controllers: PD and FPD. Even though stability was not able to guaranteed for the resting three types controllers, their identified results shows that complex controllers can generate motion trajectories which have a high fit with experiment. Identified FPD controllers have a relative smaller difference of eigenvalues among participants.

5.6 REFERENCES

[1] Arthur D Kuo. An optimal control model for analyzing human postural balance. *IEEE transactions on biomedical engineering*, 42(1):87–101, 1995.

[2] AV Alexandrov, AA Frolov, FB Horak, P Carlson-Kuhta, and S Park. Biomechanical analysis of strategies of equilibrium control during human upright standing. *Russian J Biomech*, 8(3):28–42, 2004.

[3] Chenggang Liu and Christopher G Atkeson. Standing balance control using a trajectory library. In *2009 IEEE/RSJ International Conference on Intelligent Robots and Systems*, pages 3031–3036. Citeseer, 2009.

[4] Benjamin Stephens. Humanoid push recovery. In *Humanoid Robots, 2007 7th IEEE-RAS International Conference on*, pages 589–595. IEEE, 2007.

[5] David A Winter. Human balance and posture control during standing and walking. *Gait & posture*, 3(4):193–214, 1995.

[6] Shirley Rietdyk, AE Patla, DA Winter, MG Ishac, and CE Little. Balance recov-

ery from medio-lateral perturbations of the upper body during standing. *Journal of biomechanics*, 32(11):1149–1158, 1999.

[7] Sukyung Park, Fay B Horak, and Arthur D Kuo. Postural feedback responses scale with biomechanical constraints in human standing. *Experimental brain research*, 154 (4):417–427, 2004.

[8] Torrence DJ Welch and Lena H Ting. A feedback model predicts muscle activity during human postural responses to support surface translations. *Journal of neurophysiology*, 2008.

[9] Tim Kiemel, Yuanfen Zhang, and John J Jeka. Identification of neural feedback for upright stance in humans: stabilization rather than sway minimization. *Journal of Neuroscience*, 31(42):15144–15153, 2011.

[10] RJ Peterka. Sensorimotor integration in human postural control. *Journal of neurophysiology*, 88(3):1097–1118, 2002.

[11] Adam D Goodworth and Robert J Peterka. Identifying mechanisms of stance control: a single stimulus multiple output model-fit approach. *Journal of neuroscience methods*, 296:44–56, 2018.

[12] Herman van der Kooij, Edwin van Asseldonk, and Frans CT van der Helm. Comparison of different methods to identify and quantify balance control. *Journal of neuroscience methods*, 145(1-2):175–203, 2005.

[13] Torrence DJ Welch and Lena H Ting. A feedback model explains the differential scaling of human postural responses to perturbation acceleration and velocity. *Journal of Neurophysiology*, 2009.

[14] Herman Van Der Kooij and Erwin De Vlugt. Postural responses evoked by platform

pertubations are dominated by continuous feedback. *Journal of neurophysiology*, 2007.

[15] Herman Van Der Kooij and Robert J Peterka. Non-linear stimulus-response behavior of the human stance control system is predicted by optimization of a system with sensory and motor noise. *Journal of computational neuroscience*, 30(3):759–778, 2011.

[16] Oskar Von Stryk and Roland Bulirsch. Direct and indirect methods for trajectory optimization. *Annals of operations research*, 37(1):357–373, 1992.

[17] David A Winter. *Biomechanics and motor control of human movement*. John Wiley & Sons, 2009.

[18] General information of atlas. `https://www.sympy.org/en/index.html`. Accessed: 2019-02-13.